Lunar Photometry From Clementine Multiangular Data: Analysis Of Hapke Parameters Estimate And Implication For Upcoming Smart-1 Spot-Pointing DatA. V. G. Kaydash[1,2], P. C. Pinet[1], D. Baratoux[1], S. Besse[1], A. Jehl[1], S. Chevrel[1] .[1]UMR 5562/ CNRS/ Toulouse III University, Midi-Pyrenees Observatory, 14 Av. E. Belin, 31400 Toulouse, France; [2]Astronomical Institute of Kharkov Natl. University, Sumskaya 35, Kharkov, 61022 Ukraine.

Introduction: The analysis and interpretation of reflectance dependence on illumination / observation geometry is widely used in planetary research. Two main issues are generally addressed in this field: 1) the choice of an appropriate quantitative photometric model describing the physics of the scattering by regolithic surfaces; 2) when dealing with orbital observations, how extensive should the photometric orbital survey be for a reliable derivation of the photometric function parameters? In this study we explore how well constrained is the determination of photometric function parameters using: 1) the widely used Hapke photometric model and 2) extensive set of spot-pointing observations provided by Clementine over the Reiner-Gamma region on the Moon.

Reiner-Gamma spot-pointing photometry: The well-documented photometric phase function is derived from spot-pointing observations over the Reiner-Gamma formation [1, 2, 5] known as a photometrically unusual "swirl" feature. Here, we consider the southern bright part of the swirl and the adjacent dark mare basalts southward region (inset in Fig. 1). The diversity of phase curves (for wavelength 900 nm) is also shown on Fig. 1.: blue (for the brightest part of the swirl), green – for the darkest mare basalt area and red one for the swirl part with a lower reflectance. These data offers the possibility of deriving phase curves in the range 10-80 degrees, with observations made both in and out of the principal scattering plane.

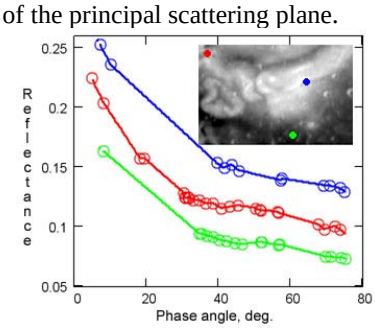

Figure 1. Examples of phase function for 3 different spots in the region of investigation.

Estimation of the photometric function parameters: Hapke photometric model for the regolith light-scattering [3] operates with 6 parameters ($B0$, h, b, c, θ, w). The opposition effect at small phase angles is described by ($B0$, h). Scattering indicatrix of regolith particles is approximated by the Henyey-Greenstein formulae leading to (b,c) quantities. Effect of macroscopic roughness of the surface is described by θ and surface single-scattering albedo by w. For the estimation of Hapke parameters, various techniques are used, such as Monte-Carlo method [4] or fast genetic algorithms [5]. A somewhat different direct approach is implemented here with the objective of assessing the reliability on the parameters determination. For this purpose, we fit the measurements with Hapke function calculated for various combinations of parameters, the four-dimensional space of parameters (b, c, θ, w) being paved with 50 grid points along each axis. Consequently, b, c, w parameters vary from 0 to 1 with a 0.02 step and from 0 to 50 degrees with 1° step for θ. Values of $B0$ and h can be reliably estimated only if an appropriate number of reflectance measurements spanning low phase angles (0-20°) is available, which is not the case here (see Fig. 1). To check the stability of opposition effect parameters estimation we have implemented varying $B0$ and h for selected points. Finally we found much dispersed values for ($B0$, h). Therefore, relying on [6], parameters $B0$ and h are set to 0.94 and 0.09, respectively. As a result, for each pixel of the image, we run 50^4 solutions and calculate for each one, the residual mean square (rms) error resulting from the phase curve fit.

Critical assessment of the Phase Function modeling and parameter determination: We rank all solutions according to the rms increase and a non-linear dependence is observed when cumulating the number of acceptable solutions, starting from the best one. We have analyzed the sequence of solutions for all cases and found that beyond the first 15-31 best solutions, the rms error increases much slower than for the first solutions case. Consequently, increasing for the sake of statistics without careful analysis the number of solutions considered acceptable when setting an upper rms threshold may be misleading as it may result for a given pixel in a progressive scatter in the distribution of solutions for a given photometric parameter. The above analysis has prompted us to build up statistics (mean and standard deviation) from the 15 best solutions for deriving Hapke parameters estimates. This fact points at the strong dependence of the fitting process on the intrinsic photometric accuracy of the data. In the present data set, the reflectance values, expressed in REFF factor, vary in the range 0.07- 0.25 and the best 15 solutions retained correspond to rms residuals less than 0.005. Depending on the data quality (i.e. SNR), it suggests that the well-constrained retrieval of Hapke parameters may not always be

achieved with orbital data. A more extensive direct approach has also been recently applied to the simulated and Mars Express HRSC orbital data [7]. It shows how the accuracy of observational data affects estimates of Hapke parameters; which in some cases may become non-constrained with solutions scattered across most of the parametric space (see details in [7]).

Fig. 2. shows scatter plot diagrams (*c*, *b*) and (θ, *w*) (in red) with corresponding standard deviations (in blue). The well-known L-shaped (*c*, *b*) diagram has been noted in several works (e.g. [8]) and the present study agrees with these earlier results. The frequency distribution histogram for *c* parameter is bimodal with the first mode centered at ~ 0.15 (swirl area) and second one ~0.4 for mare regolith. The roughness θ is also bimodal (θ<25 deg. for mare region vs. θ>25 deg. for Reiner-Gamma). We also find the θ versus *w* trend that has been previously reported together with θ diversity for mare vs. swirl [5], calling for some (θ, *w*) interchangeability [11]. These results generally agree with results produced from inverse modeling [5, 10].

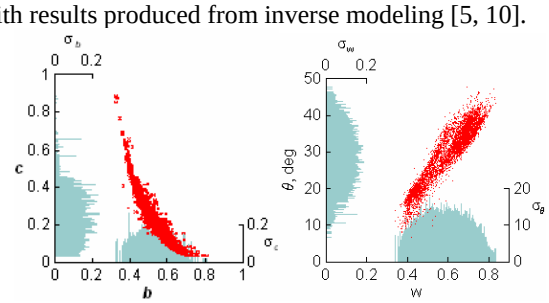

Figure 2. Scatter plot diagrams and standard deviations: Full phase curve case.

However, we note that the standard deviations σ_b, σ_c, σ_w for Hapke parameters may range up to 0.2 for *b*,*c*,*w* and up to 12 deg. for θ. It indicates that the parameters determination is not always fully constrained.

Implication for derived-photometry from limited phase coverage: Upcoming ESA SMART-1 spot-pointing mission phase should allow for lunar imaging photometry with AMIE camera [9] and phase angles coverage will vary depending on the illumination and geometry conditions. In order to assess the consequence of limited phase range measurements on the determination of Hapke parameters, we have performed two experiments with degraded phase curves using the same direct approach described above.

Case 1: Phase coverage 40-80 degrees. Excluding the low phase angle reflectance values from the fitting process disturbs the L-shaped (*c*, *b*) dependence, with a strong *b* variation for the mid-range *c* values as shown on Fig. 3, and σ_b and σ_c reaching 0.2-0.3. The direct correlation (θ, *w*) is also deteriorated although σ_b and σ_c decrease for a given (θ, *w*) pair.

Case 2: Phase coverage 10-50 degrees. Conversely, as shown on Fig. 4, considering only the low phase angle reflectance values causes all the (*c*, *b*) pairs for image points to fall in the L-shaped dependence with rather low (σ_b, σ_c) values. The whole region appears then characterized by low *c* (<0.5) values with *b* almost in the same range as in the case of the full phase curve case (see Fig. 3) while the frequency distribution for θ becomes blockier and unimodal.

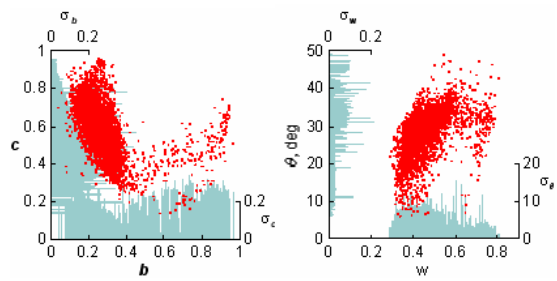

Figure 3. Scatter plot diagrams and standard deviations: 40-80 degrees phase curve case.

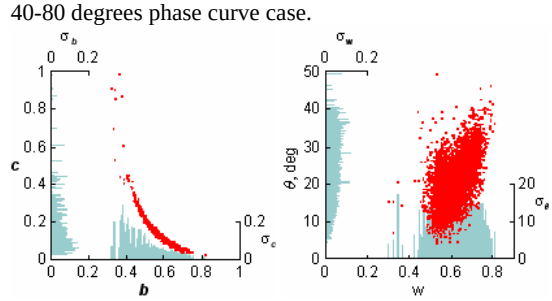

Figure 4. Scatter plot diagrams and standard deviations: 10-50 degrees phase curve case.

Conclusion: A degraded phase function results in an alteration of derived Hapke parameters, either for low or high phase angle measurements, and may lead to incorrect interpretation of the surface scattering properties (see also [7]). We thus recommend for AMIE observation to cover as wide a range of phases as possible, with a discrete number (7-10) of geometric configurations to be acquired either along-track or across-track from separate orbits, depending on the latitude of the selected targets to be surveyed.

References: [1] Kreslavsky et al,. (2000), *J.Geophys. Res.*, 105, 20281. [2] Pinet et al,. (2000), *J.Geophys. Res.*, 105, 9457. [3] Hapke B. (1993) Cambridge Univ. Press. [4] Hillier, J. and Buratti, B. (2001) *Icarus*, 149, 251. [5] Pinet P.C. et al. (2004) *LPS XXXV*, Abstract #1660. [6] Hillier et al., (1999), *Icarus*, 141. 205. [7] Baratoux, D. et al. (2006) *LPSC XXXVII*, This volume. [8] McGuire, Hapke, (1995), *Icarus*, 113, 134. [9] Pinet, P. et al. (2005), *Plan. Space. Sci.* V. 53, 13, 1309. [10] Chevrel, S. et al. (2006) *LPSC XXXVII*, this volume. [11] Shkuratov, Y. et al. (2005), *Icarus*, 173, 3.